

OPEN ACCESS

Vacancy clusters in ultra fine grained metals prepared by severe plastic deformation

To cite this article: J Čížek *et al* 2013 *J. Phys.: Conf. Ser.* **443** 012008

View the [article online](#) for updates and enhancements.

You may also like

- [Study on low intensity aeration oxygenation model and optimization for shallow water](#)
Xiao Chen, Zhibin Ding, Jian Ding et al.
- [Comparative Study of PID, Type-1 and Type-2 Fuzzy Control for Nonlinear Systems](#)
Yao Chen, Jiahao Liu and Tao Zhao
- [Stability Assessment of an Eco-Industrial System Based on Entropy Analysis Method](#)
Feng Han, Dong Yang and Feng Shi



ECS
The
Electrochemical
Society
Advancing solid state &
electrochemical science & technology

DISCOVER
how sustainability
intersects with
electrochemistry & solid
state science research

Vacancy clusters in ultra fine grained metals prepared by severe plastic deformation

J. Čížek¹, O. Melikhova¹, Z. Barnovská¹, I. Procházka¹, R. K. Islamgaliev²

¹Charles University in Prague, Faculty of Mathematics and Physics,
V Holešovičkách 2, 180 00 Prague 8, Czech Republic

²Institute of Physics of Advanced Materials, Ufa State Aviation Technical University,
12 K. Marx Street, 450000 Ufa, Russian Federation

E-mail: jakub.cizek@mff.cuni.cz

Abstract. Severe plastic deformation of metals introduces not only dislocations, but also a high concentration of vacancies. In the present work we employed positron lifetime spectroscopy for investigation of deformation-induced vacancies in ultra fine grained metals prepared by high pressure torsion. It was found that in all metals studied deformation-induced vacancies agglomerate into small vacancy clusters. Experimental positron lifetime results were combined with *ab-initio* theoretical calculations of positron parameters for vacancy clusters of various sizes. This new approach described in this paper enables to determine the size distribution of vacancy clusters.

1. Introduction

Severe plastic deformation (SPD) enables to achieve an extreme grain refinement down to nanoscopic dimensions leading to formation of ultra fine grained (UFG) structure. SPD introduces a high density of dislocations into the strained material. Moreover, non-conservative movement of dislocations leads to formation of vacancies. An indirect evidence for deformation-induced vacancies in UFG metals comes from comparison of differential scanning calorimetry (DSC) and electrical resistivity with X-ray diffraction (XRD) line profile analysis [1,2]. Dislocation densities determined by DSC from the total stored energy and by electrical resistivity are significantly higher than those obtained by XRD [2]. This discrepancy can be explained by excess vacancies, which also contribute to the total stored energy and electrical resistivity, but do not cause broadening of XRD profiles. Direct evidence for deformation-induced vacancies in UFG Cu and Ni was obtained by positron annihilation spectroscopy [3,4]. Since in majority of metals vacancies are mobile at room temperature, some fraction of deformation-induced vacancies disappear by diffusion to sinks at grain boundaries, while other vacancies agglomerate and form small vacancy clusters which are more stable than single vacancies. Driving energy for this process is reduction of the surface energy of vacancies.

Among the variety of SPD-based techniques, the high pressure torsion (HPT) [5] leads to the strongest grain refinement. For this reason HPT was chosen for preparation of UFG samples studied in the present work. The deformation-induced vacancy clusters in various UFG metals with fcc, bcc and hcp structure were investigated by positron lifetime (LT) spectroscopy combined with *ab-initio* theoretical calculations. This approach enables to determine the size distribution of deformation-induced small vacancy clusters.



2. Experimental

A digital spectrometer [6] with excellent time resolution of 145 ps (FWHM ^{22}Na) was employed for LT investigations. At least 10^7 annihilation events were accumulated in each LT spectrum. A $^{22}\text{Na}_2\text{CO}_3$ positron source with activity of ~ 1 MBq deposited on a 2 μm thick mylar foil was always sealed between two identical pieces of sample. Diameter of the source spot was ~ 3 mm. The source contribution which comes from positrons annihilated in the source spot and the covering mylar foil consisted of two weak components with lifetimes of 0.368 and 1.5 ns.

Specimens of well annealed Cu (99.95%), Al (99.9999%), Fe (99.99%), Nb (99.9%), W(99.95%), and Ti (99.7%) were subjected to quasi-constrained HPT straining under pressure of 6 GPa. The samples were strained by 5 HPT revolutions performed at 450°C (W), 150°C (Nb) and at room temperature (Cu, Al, Fe, Ti). The grain size determined by transmission electron microscopy falls in the range 100-250 nm for all samples studied except of Al which exhibits the mean grain size of ~ 0.5 μm . HPT-deformed specimens were disk shaped, with a diameter of ~ 10 mm and a thickness of ~ 0.3 mm. LT investigations were always performed in the centre of the sample disk except of HPT-deformed Cu where LT characterizations were done not only in the centre but also at the periphery with positron source positioned at the radial distance $r = 3$ mm from the centre.

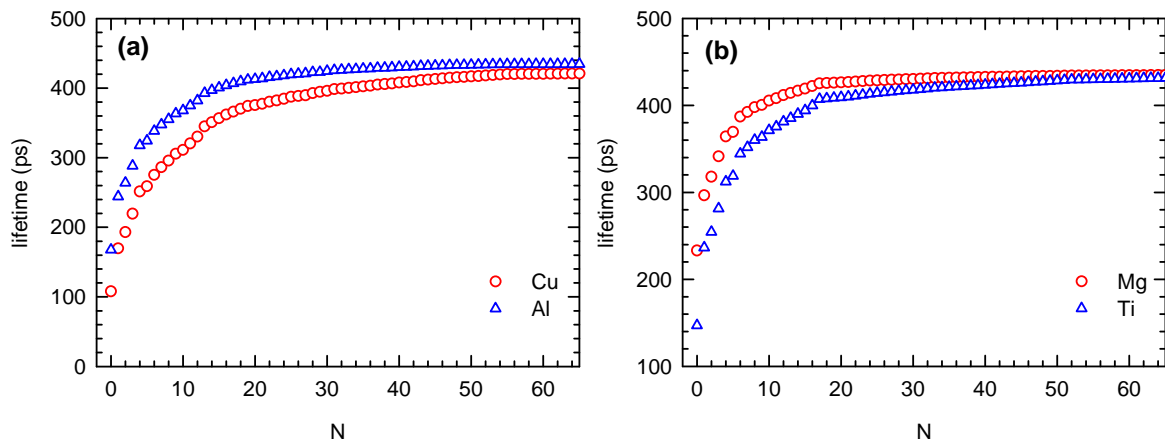


Figure 1. Calculated dependence of the positron lifetime on the size of vacancy clusters consisting of N vacancies: (a) fcc metals Cu, Al; (b) hcp metals Mg, Ti.

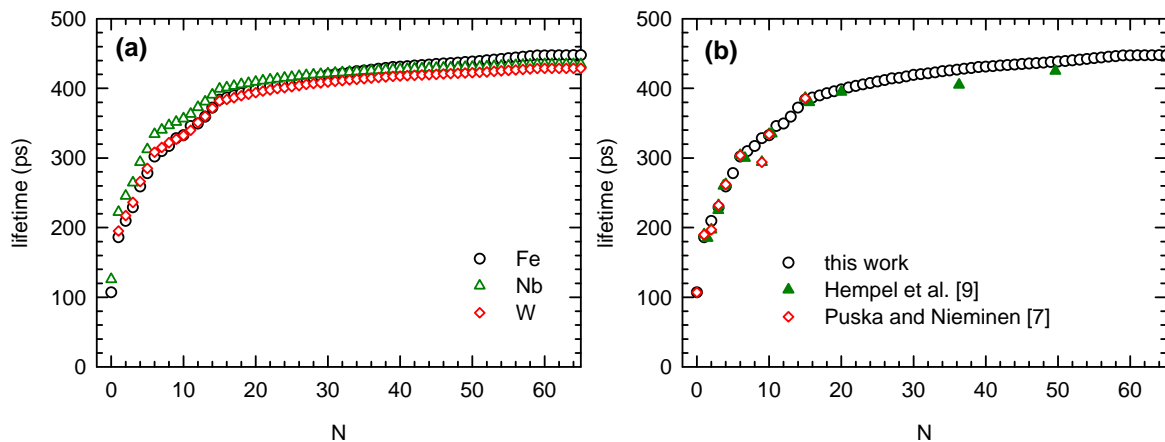


Figure 2. (a) Calculated dependence of the positron lifetime on the size of vacancy clusters consisting of N vacancies for bcc metals Fe, Nb, W; (b) Comparison of the lifetimes calculated in this work for Fe with data existing in literature.

3. Theoretical calculations

Theoretical calculations of positron lifetimes were performed within the so-called standard scheme employing the atomic superimposition (ATSUP) method for construction of electron density [7]. The electron–positron correlations were treated according to Boroński and Nieminen [8]. The calculations have been done in 512 atom-based supercells. Vacancies were introduced simply by removing corresponding atoms from the supercell. Equilibrium geometry of vacancy clusters was obtained by minimizing their surface. No atomic relaxations were considered in the present stage of calculations.

Calculated lifetimes of positrons trapped at vacancy clusters consisting of N vacancies are plotted in Fig. 1(a) and 1(b) for fcc metals (Al, Cu) and hcp metals (Mg, Ti), respectively. Calculated positron lifetimes for metals with bcc structure (Fe, Nb, W) are plotted in Fig. 2(a). Positron lifetime firstly strongly increases for very small clusters, while for larger clusters it gradually saturates. Theoretical calculations of positron lifetimes for selected vacancy clusters in Fe were performed in Refs. [7,9]. These results which are plotted in Fig. 2(b) are in a satisfactory agreement with our calculations.

Table 1. Results of LT measurements of HPT deformed metals.

Fit using discreet components only

Sample	τ_1 (ps)	I_1 (%)	τ_2 (ps)	I_2 (%)	τ_3 (ps)	I_3 (%)	χ^2 / n
Cu	-	-	164(1)	76.0(6)	256(2)	24.0(5)	1.06
Al	149(8)	71(5)	252(9)	26(1)	450(50)	3(1)	1.03
Fe	-	-	150.8(6)	91.1(4)	360(9)	8.9(4)	1.07
Nb	-	-	173.9(8)	94(1)	300(10)	6(1)	1.10
W	-	-	160.8(6)	90.8(4)	367(7)	9.2(7)	1.04
Ti	-	-	185.2(5)	98.4(7)	430(70)	1.6(7)	1.05

Fit using size distribution of vacancy clusters, Eq. (1)

Sample	τ_1 (ps)	I_1 (%)	τ_2 (ps)	I_2 (%)	ν_d	I_d (%)	χ^2 / n
Cu	-	-	164(1)	73.3(8)	3.7(2)	26.7(8)	1.03
Al	158(1)	86.5(4)	240(3)	10(1)	40(3)	3.5(4)	1.02
Fe	-	-	150.8(8)	89.8(2)	11.3(5)	10.2(3)	1.03
Nb	-	-	174(1)	91.2(3)	3.0(2)	8.8(5)	1.04
W	-	-	161.6(6)	90.5(5)	13(1)	9.5(7)	1.02
Ti	-	-	182(1)	96.3(5)	39(2)	3.7(7)	1.03

4. Results and discussion

The LT spectra of HPT-deformed metals with exception of Al consist of two components, see Table 1. The lifetime τ_2 of the shorter component is slightly shorter compared to that for a monovacancy [10] which is typical for dislocations. It is well known that dislocation line itself is only a shallow positron trap [11]. Positron pre-trapped at a dislocation diffuses quickly along the dislocation line until it becomes finally confined at a deep trap provided by a vacancy anchored in the compressive elastic field of dislocation [11]. Hence, positron is finally annihilated in a vacancy squeezed by the elastic field of dislocation resulting in lifetime slightly shorter than that for a bare monovacancy. In case of HPT-deformed Al a short lived free-positron component with lifetime τ_1 was observed in addition to the dislocation component. This indicates a dynamic recovery of UFG structure during HPT processing, which was observed also in HPT-deformed Mg [12]. In other metals studied the concentration of defects is high enough to cause saturated positron trapping.

All HPT-deformed metals studied exhibit a long-lived component with lifetime τ_3 (see Table 1) which comes from positrons trapped at vacancy clusters. The mean size of vacancy clusters can be

estimated by comparison of the lifetime τ_3 with the theoretical calculations in Figs. 1, 2. However, HPT-deformed metals contain obviously certain size distribution $P(N)$ of deformation-induced vacancy clusters. Hence LT spectrum of a HPT-deformed metal can be assumed in a general form

$$S(t) = \left\{ \sum_i \frac{I_i}{\tau_i} e^{-\frac{t}{\tau_i}} + I_d \left(\sum_N v_N \right)^{-1} \sum_N \frac{v_N}{\tau_N} P(N) e^{-\frac{t}{\tau_N}} \right\} \otimes R(t) + B, \quad (1)$$

where τ_i , I_i denotes the lifetimes and the relative intensities of discrete exponential components, here the free positron component ($i = 1$), if present, and the dislocation component ($i = 2$). The symbol I_d denotes the relative intensity of the cluster contribution given by a superposition of exponential components with lifetimes τ_N of positrons trapped at vacancy clusters consisting of N vacancies. These lifetimes were obtained from theoretical calculations in Figs. 1, 2. Each component is weighted by a factor $v_N P(N)$, where v_N is the specific positron trapping rate accounting for varying cross-section for positron trapping at vacancy clusters of various size. For small vacancy clusters ($N \leq 10$) v_N is proportional to the cluster size, while for larger clusters the slope of this dependence decreases. Nieminen and Laakkonen [13] calculated v_N for vacancy clusters of various sizes in Al. From interpolation of these results the dependence of v_N on the cluster size can be approximated as $v_N / v_1 \approx 9.4 (1 - e^{-0.13 N})$. The ideal spectrum in brackets in Eq. (1) is convoluted with the resolution function $R(t)$ of the spectrometer and a constant background B from random coincidences is added. The relative intensities and size distribution of vacancy clusters always satisfy the normalization conditions

$$\sum_i I_i + I_d = 1 \quad \text{and} \quad \sum_N P(N) = 1. \quad (2)$$

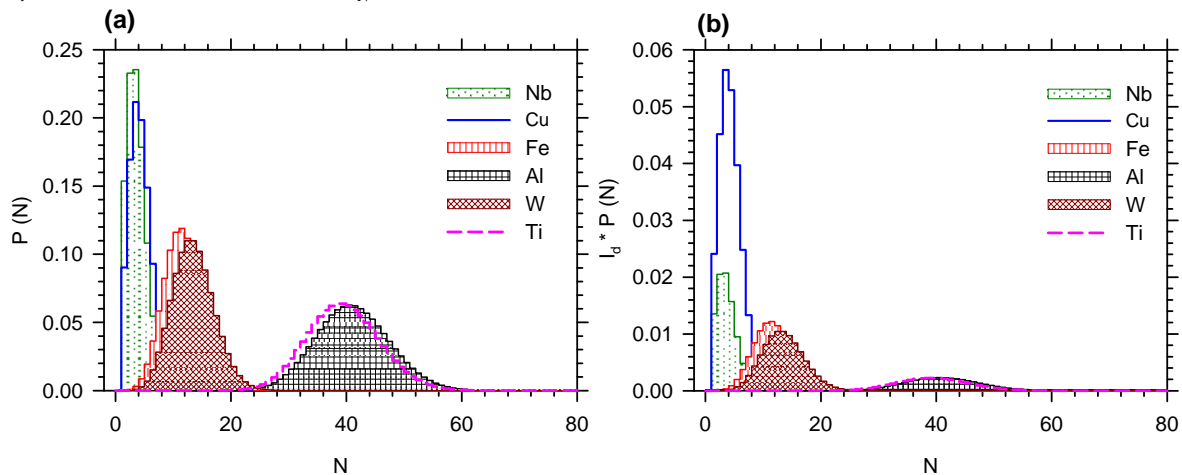


Figure 3. (a) The size distribution $P(N)$ of vacancy clusters in various HPT-deformed metals; (b) the size distribution $P(N)$ of vacancy clusters multiplied by the relative intensity I_d of the cluster contribution. All results were measured at the centre of the sample disks.

Vacancy clusters are created by agglomeration of deformation-induced vacancies. Movement of a screw dislocation with a jog results in creation of a row of vacancies or interstitial atoms. The creation of vacancies dominates due to their lower formation energy. Hence, vacancies are introduced in rows created by moving dislocation. Since vacancy clusters are formed by agglomeration of vacancies in these rows, the size of vacancy clusters depends predominantly on the number of vacancies in these rows. Drag of a dislocation jog is result of many attempts to move the jog under applied stress. Hence the number of vacancies in the row created by a jog dragged by moving dislocation can be described by the Poisson distribution

$$P(N) = \frac{v^N e^{-v_d}}{N!}, \quad (3)$$

where ν_d is the mean size vacancy clusters. The second part of Table 1 shows result of fitting of LT spectra by Eq. (1) with $P(N)$ given by Eq. (3). It was found that such model function describes the experimental data accurately in all metals studied. Since we use the Poisson distribution $P(N)$ with the only fitting parameter ν_d (the variance of the distribution equals to the mean) the model function given by Eq. (1) does not introduce any new fitting parameter compared to the conventional approach with discrete components. Last column in Table 1 shows the χ^2 coefficient per the number of degrees-of-freedom n . Obviously fitting of LT spectra by Eq. (1) improved χ^2 coefficient with respect to the conventional model with discrete components in case of all samples except of Al where it remains the same. Moreover, in Al the fitting by Eq. (1) resulted in lifetime τ_2 which agrees better with lifetime of positrons trapped at dislocations in Al [14]. Fig. 3(a) shows the distributions $P(N)$ (normalized to the unit area) obtained from fitting of LT spectra. The distributions multiplied by the relative intensity I_d of the cluster contribution are plotted in Fig. 3(b). The latter distributions give information not only about the size distribution of vacancy clusters, but also about their concentration. Cu and Nb exhibit very narrow size distribution of vacancy clusters with the mean size of ~ 4 vacancies, Fe and W contain larger vacancy clusters with the mean size of ~ 10 vacancies, Al and Ti contain the biggest vacancy clusters with the mean size of ~ 40 vacancies having a wide size distribution. The size distribution of vacancy clusters in HPT-deformed metals is not directly related to their crystalline structure, e.g. fcc Cu exhibits very small clusters while fcc Al contains big clusters. Systematic investigations on a broader set of UFG metals are required to identify the factors influencing the size distribution of deformation-induced clusters. However, it seems to be clear that the majority of vacancy clusters is not formed directly by deformation, but rather by aggregation of deformation-induced vacancies. Since the accumulation rate is influenced by the mobility of vacancies the big clusters in Al and Ti are likely formed due to low activation energy E_m for migration of vacancies in these two metals. Theoretical calculations revealed $E_m = 0.43$ eV [15] and 0.42 eV [16] for Ti and Al, respectively, which is less than half of the vacancy migration energy in Cu, $E_m = 1.00$ eV [17].

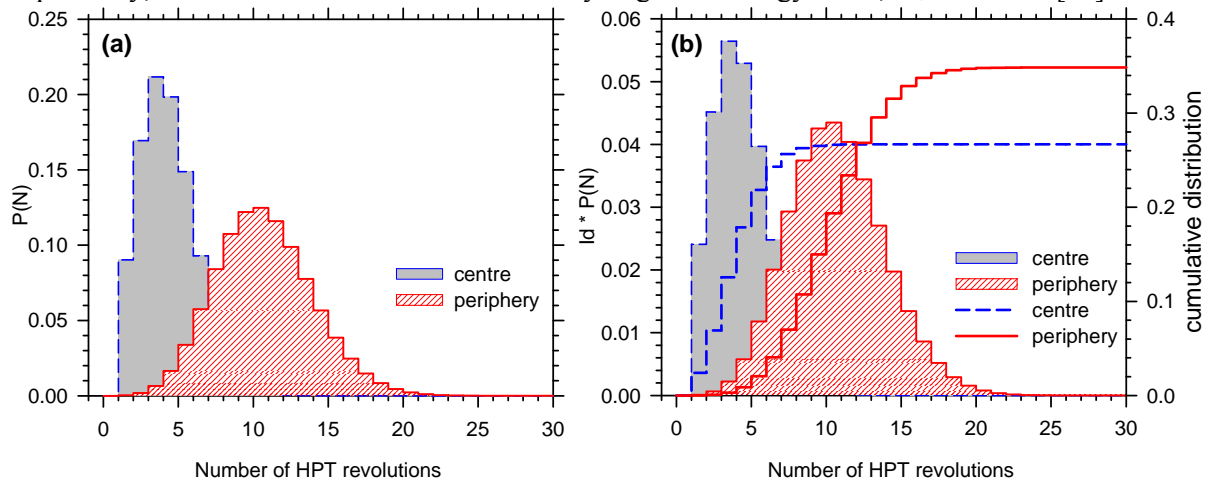


Figure 4. Comparison of the size distribution of vacancy clusters in UFG Cu in the centre of the sample ($r = 0$) and at the periphery ($r = 3$ mm): (a) comparison of the normalized size distribution $P(N)$; (b) the size distribution $P(N)$ multiplied by the relative intensity I_d of the cluster component. Thick lines show cumulative distribution $I_d \sum P(N)$.

The vacancy production rate at low temperature plastic deformation depends on the strain rate $\dot{\epsilon}$ [18]

$$\Pi = \alpha \frac{\sigma \Omega_0}{E_f} \dot{\epsilon}, \quad (4)$$

where the coefficient $\alpha \approx 0.1$ [19], σ is the applied stress, Ω_0 the atomic volume and E_f the vacancy formation energy. In torsion deformation the strain rate increases with the radial distance r from the centre of the sample (corresponding to the rotation axis). The results given in Table 1 and Fig. 3 were

obtained with the positron source positioned at the centre of the sample. Since all samples studied were deformed in the same way, the strain rate was identical for all samples. The diameter of the central area of the sample probed by positrons is approximately 3 mm due to finite size of the source spot. To examine the influence of strain rate on the size distribution of vacancy clusters UFG Cu sample was measured not only at the centre but also at the “periphery” with the positron source located at the distance $r = 3$ mm from the centre. A comparison of the size distribution of vacancy clusters measured at the centre and at the periphery is given in Fig. 4(a). Obviously the vacancy clusters at the periphery are larger compared to those in the centre due to higher production rate of vacancies. The size distribution $P(N)$ multiplied by the relative intensity I_d of the cluster distribution is plotted in Fig. 4(b) together with the cumulative distribution $I_d \sum_N P(N)$. The total concentration of deformation-induced vacancies is clearly higher at the periphery because of higher strain rate.

5. Conclusions

SPD introduces a lot of vacancies which subsequently agglomerate into clusters. Size distribution of these deformation-induced clusters in various UFG metals prepared by HPT was determined by LT spectroscopy combined with *ab-initio* theoretical calculations. It was found that size distribution of vacancy clusters is considerably different in various UFG metals. A high mobility of vacancies in Al and Ti leads to formation of rather big clusters with mean size of ~ 40 vacancies and wide size distribution, Fe and W exhibit smaller vacancy clusters with size of ~ 10 vacancies, very small clusters with size of ~ 4 vacancies and narrow size distribution were found in Cu and Nb. Vacancy clusters at the periphery of the sample disk are larger compared to those in the centre due to higher strain rate.

6. References

- [1] Schafler E, Steiner G, Korznikova E, Kerber M and Zehetbauer M 2005 *Mater. Sci. Eng. A* **410-411** 169
- [2] Ungar T, Schafler E, Hanák P, Bernstorff S and Zehetbauer M 2007 *Mater. Sci. Eng. A* **462** 398
- [3] Čížek J, Janeček M, Srba O, Kužel R, Barnovská Z, Procházka I and Dobatkin S 2011 *Acta Mater.* **59** 2322
- [4] Oberdorfer B, Steyskal E-M, Sprengel W, Puff W, Pikart P, Hugenschmidt Ch, Zehetbauer M, Pippan R and Würschum R 2010 *Phys. Rev. Lett.* **105** 146101
- [5] Zhilyaev A P and Langdon T G 2008 *Prog. Mater. Sci.* **53** 893
- [6] Bečvář F, Čížek J, Procházka I and Janotová J 2005 *Nucl. Instrum. Methods A* **539** 372
- [7] Puska M J and Nieminen R M 1983 *J Phys F* **13** 333
- [8] Boroński E and Nieminen R M 1983 *Phys Rev B* **34** 3820
- [9] Hempel A, Hasegawa M, Brauer G, Plazaola F, Saneyasu M and Tang Z 1999 *Proc. of the 9th Int. Conf. on "Environmental Degradation of Materials in Nuclear Systems-Water Reactors"*, (Aug. 1-5, 1999, Newport Beach, CA, USA)
- [10] Campillo Robles J M, Ogando E and Plazaola F 2007 *J. Phys.: Condens. Matter* **19** 176222
- [11] Smedskjaer L, Manninen M and Fluss M 1980 *J. Phys. F: Met. Phys.* **10** 2237
- [12] Čížek J, Procházka I, Smola B, Stulíková I, Kužel R, Matěj Z, Cherkaska V, Islamgaliev R K and Kulyasova O 2005 *Mater. Sci. Forum* **482** 183
- [13] Nieminen R M and Laakkonen J 1979 *Appl. Phys.* **20** 181
- [14] Petersen K, Repin I A and Trumpy G 1996 *J. Phys.: Condens. Matter* **8** 2815
- [15] Verite G, Willaime F and Fu Ch-Ch 2007 *Solid State Phenomena* **129** 75
- [16] Da Fano A and Jacucci G 1977 *Phys. Rev. Lett.* **39** 950
- [17] Plishkin Yu M and Podchinenov I E 2006 *Phys. stat. sol. (a)* **38** 51
- [18] Militzer M, Sun W P and Jonas J J 1993 *Acta Mater.* **42** 133
- [19] Gottstein G, Bewerunge J, Mecking H and Wollenberger H 1975 *Acta Met.* **23** 641

Acknowledgments

This work was supported by the Czech Science agency (project P108/12/G043).